Special Perforated Steel Plate Shear Walls with Reduced Beam Section Anchor Beams. I: Experimental Investigation

Darren Vian, M.ASCE[1]; Michel Bruneau, M.ASCE[2]; K. C. Tsai[3]; and Y.-C. Lin[4]

Abstract: This paper presents results of an experimental investigation of specially detailed ductile perforated steel plate shear walls (SPSWs) designed to accommodate utility passage, and having anchor beams with reduced beam sections connections. Single-story, single-bay SPSW frames are subjected to quasi-static cyclic loading up to their maximum strength and displacement capacity. The tested specimens also had low yield strength steel infill panels. Two specimens make allowances for penetration of the panel by utilities. The first, having multiple holes specially laid out in the steel panel, also has the characteristic of reduced panel strength and stiffness compared to the corresponding SPSW having a solid panel. The second such specimen utilizes quarter-circle cutouts in the panel corners, which are reinforced to transfer the panel forces to the adjacent framing. A SPSW with solid panel is also tested for reference purposes. All specimens resisted an imposed input history of increasing displacements to a minimum drift of 3%. The perforated panel reduced the elastic stiffness and overall strength of the specimen by 15% as compared with the solid panel specimen.

DOI: 10.1061/(ASCE)0733-9445(2009)135:3(211)

CE Database subject headings: Steel plates; Beams; Anchors; Experimentation; Shear walls.

Introduction

The use of steel plate shear walls (SPSWs) as the lateral force resisting system in building has become significantly more popular in North America and Asia in recent years. Since the early 1980s, SPSW research has advocated the use of relatively thin plates for the infill panels, an approach that allows for the occurrence of panel shear buckling and subsequent development of diagonal tension field action as the method of lateral load resistance and transmission to the boundary frame, and that makes SPSWs an economically viable alternative.

Seismic design requirements for SPSW design were introduced in the recent editions of the AISC seismic design guidelines (AISC 2005b) and the FEMA 450 (FEMA 2003) recommended guidelines for seismic design, bringing the system into broader acceptance as a design option. Nonetheless, some obstacles still exist that may impede more widespread usage of this system in the design community. For example, for low-rise buildings, the SPSW infill panel thicknesses required to resist specified lateral loads are often less than the minimum panel thickness available from steel producers for hot rolled plate grades typically available in North America. In such cases, use of the minimum available thickness may result in large panel force overstrengths. Attempts at alleviating this problem were recently addressed by the use of light-gauge, cold-formed steel panels, in a new application by Berman and Bruneau (2003a, 2005). Xue and Lu (1994) suggested additional means of reducing demand on framing adjacent to an SPSW, including the connection of the infill panel to only the beams in a moment frame.

The practical concern of utility placement is another impediment to more widespread acceptance of the SPSW structural system. If the SPSW infill panel occupies an entire frame bay between adjacent beams and columns, then utilities that may have otherwise passed through that location must either be diverted to another bay, or pass through a heavily stiffened opening, as prescribed in current design codes. This would add costs to the project in either additional materials (for the extra stiffening) or in labor (for the relocation of ductwork in a retrofit, for example). Therefore, more work is required to ensure the viability of the SPSW system over a wide range of situations to make it more acceptable to design engineers.

This paper investigates new methods for the design of special perforated ductile SPSWs. Two approaches to alter the solid infill panel system to allow for the passage of utilities through the plane of the wall are considered. One system accomplishes this goal using a special panel perforations layout, which, in addition to allowing utility pass through, may be used to reduce the strength and stiffness of a solid panel wall to levels required in a design when a thinner plate is unavailable. Another system preserves the general strength and stiffness of a solid SPSW panel, while allowing utility passage through a reinforced cutout that transmits panel forces to the boundary frame. In addition, in all cases, reduced beam sections (RBSs) are introduced in the SPSW "anchor" beams (those at the top and bottom ends of a SPSW). The objective of this proposed anchor beam design is to ensure that frame plastic hinging occurs at beam ends (not within beam span, or in columns).

The design concepts are verified and studied further by means of a series of approximately half-scale test specimens, subjected

[1]Structural Engineer, Parsons Brinckerhoff, New York, NY 10119. E-mail: Vian@pbworld.com; formerly, Graduate Research Assistant, Dept. of CSEE, Univ. at Buffalo, Amherst, NY 14260.

[2]Professor, Dept. of CSEE, Univ. at Buffalo, Amherst, NY 14260. E-mail: bruneau@buffalo.edu

[3]Director, NCREE, Professor, Dept. of Civil Engineering, National Taiwan Univ., Taipei, Taiwan 10617.

[4]Graduate Student, Dept. of Civil Engineering, National Taiwan Univ., Taipei, Taiwan 10617.

Note. Associate Editor: Benjamin W. Schafer. Discussion open until August 1, 2009. Separate discussions must be submitted for individual papers. The manuscript for this paper was submitted for review and possible publication on June 22, 2007; approved on November 5, 2008. This paper is part of the ***Journal of Structural Engineering***, Vol. 135, No. 3, March 1, 2009. ©ASCE, ISSN 0733-9445/2009/3-211–220/$25.00.

to quasi-static, displacement controlled, cyclic loading. A typical single story, single bay frame with solid SPSW infill panel is designed and compared with specimens implementing the perforated panel and reinforced cutout design concepts.

Literature Review

There have been numerous experimental and analytical studies investigating the behavior of unstiffened SPSWs in the past 30 years. An extensive summary of relevant research on SPSWs to date has been presented in Sabelli and Bruneau (2006).

Behavior of such SPSWs relies on the development of yielding diagonal strips from tension field action. As a result, Thorburn et al. (1983) developed a simple analytical "strip" model to represent the tension field action of a thin steel wall subjected to shear forces. This model was developed by idealizing the panel as a series of diagonally oriented "truss elements" (i.e., resisting only axial force effects). This model was verified and refined by the tests of Timler and Kulak (1983) and has been implemented into the Canadian design codes (CAN/CSA 2001) and the AISC (2005b) seismic design specifications.

Berman and Bruneau (2003a,b) investigated, using the strip model as a basis, the use of plastic analysis as an alternative for the design of steel plate shear walls. Fundamental plastic collapse mechanisms were described for single story and multistory SPSW with either simple or rigid beam-to-column connections, and the ultimate strengths predicted from these mechanisms were compared with experimental results from the literature and used to assess the CAN/CSA S16-01 design procedure. This approach allows us to quantify the entire system strength and relative contributions of frame and panel to total strength. Plastic analysis of SPSWs was further extended by the researchers to multistory frames for examples of collapse mechanisms. These mechanisms and their corresponding ultimate strengths provide the design engineer simple tools for estimating the ultimate capacity of a multistory SPSW frame, and investigating possible soft story mechanisms. Pushover analysis using the strip model was further recommended to discern the actual failure mechanisms in a given structure and aid in design as necessary.

Little literature has investigated the cyclic performance of SPSWs having perforations. Roberts and Sabouri-Ghomi (1992) conducted a series of quasi-static cyclic loading tests on unstiffened steel plate shear panels with centrally placed circular openings and proposed an approximate strength and stiffness reduction factor for a perforated panel. They determined that results for strength and stiffness of a perforated panel can be conservatively approximated by applying this reduction factor to the strength and stiffness of a similar, unperforated panel. No literature was found on the seismic performance of SPSWs with panels having multiple perforations, although behavior could be inferred by extrapolation of the Roberts and Sabouri-Ghomi study. Further, although much literature exists on connection plates having a large number of bolt holes, these plates are not designed to develop diagonal buckling and tension field of the type expected in SPSW.

Design Considerations for Anchor Beams

In a multistory building utilizing an SPSW lateral force resisting system, the primary purpose of the top and bottom beams, at roof and ground (or basement) levels, respectively, is to "anchor" the vertical component of the SPSW infill panel tension field forces. Therefore, these beams may be referred to as "anchor beams," and their design deserves special attention. To promote the use of fully fixed connections at the end of SPSW anchor beams to resist larger panel forces, while aiming for their more optimal design, it was proposed to design anchor beams by locally reducing the beam end moment strength through the use of RBS connections—that have been introduced for the design of special moment resisting frames and their detailing fully described in AISC 358 (AISC 2005a) and FEMA 350 (FEMA 2000). This detailing was, therefore, implemented in the experimental program described below.

It can be shown (Vian and Bruneau 2005), using plastic analysis, that an efficiently designed anchor beam should have a plastic modulus Z_{xab}, satisfying the following relation:

$$M_p = Z_{xab} \cdot F_{yab} \geqslant \frac{\omega \cdot L^2}{8} \cdot \left[\frac{2}{1 + \sqrt{1 - \beta^2}} \right] \tag{1}$$

where an RBS beam-to-column connection is used at each beam end and β=ratio of the plastic modulus at the RBS location Z_{RBS} to that of the gross beam section Z_{xab}; F_{yab}=yield stress of the anchor beam; L=length of the anchor beam; and ω=distributed load representing the vertical component of the panel tension field forces perpendicular to the beam, which can be related to the panel properties by

$$\omega = F_{yp} \cdot t \cdot \cos^2 \alpha \tag{2}$$

where t=panel thickness; F_{yp}=panel yield stress, assuming elastic perfectly plastic material; and α=angle of orientation, with respect to vertical, of the panel uniform tension field stresses, which is typically taken as 45° in the initial design stage, or calculated directly using an equation derived by Timler and Kulak (1983) and provided in the AISC seismic provisions (AISC 2005b). An expression for the required beam plastic modulus Z_{xab} is obtained by substituting Eq. (2) into Eq. (1) and solving for the beam plastic modulus Z_{xab}

$$Z_{xab} \geqslant \frac{L^2 \cdot t \cdot \cos^2 \alpha}{4} \cdot \frac{F_{yp}}{F_{yab}} \cdot \left[\frac{1}{1 + \sqrt{1 - \beta^2}} \right] \tag{3}$$

Design of Experimental Program

A program of quasi-static cyclic testing of SPSW specimens was developed to examine two utility-accommodating concepts, as well as the RBS anchor beam detailing concept discussed above. A "reference" specimen, "S2" consists of a single-bay, single-story frame, with RBS beam-to-column connections, and a solid infill panel of low yield strength (LYS) steel, with material properties as described in a later section below. The second specimen, "P" introduces multiple regularly spaced holes (perforations) into the panel, while the third, "CR" introduces reinforced quarter-circle cutouts in the upper corners of the panel.

Testing was conducted at the National Center for Research on Earthquake Engineering (NCREE) in Taipei, Taiwan. LYS steel, which is becoming more widely available in Asia, was used for the specimen infill panels (as a strategy to avoid the undesirable plate overstrength that occurs when the required plate thickness is less than the minimum available for hot rolled steel, as described earlier). Four static MTS (Eden Prairie, MN) hydraulic actuators, having maximum force and displacement output of 1,000 kN and 500 mm, respectively, were used to laterally load the specimens.

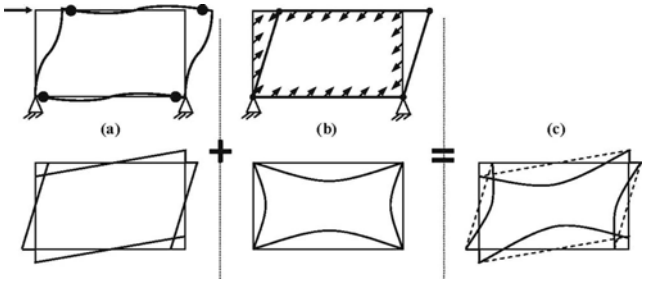

Fig. 1. Force and moment diagrams: (a) frame without infill panel; (b) rigid pin-ended frame members with SPSW panel; and (c) combined system

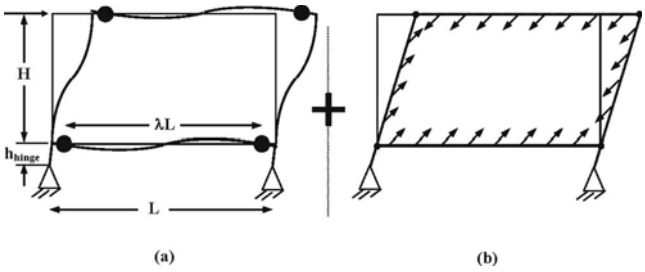

Fig. 2. Force and moment diagrams used in specimen design: (a) frame; (b) frame with rigid pin-ended members and SPSW infill panel

SPSWs specimen dimensions were 4,000 mm width by 2,000 mm height (centerline to centerline), designed to approximate half-scale of prototypes that could be used in a bay of the Multidisciplinary Center for Earthquake Engineering Research (MCEER) demonstration hospital (Yang and Whittaker 2002). Fig. 1 illustrates the assumed deformed shape of an SPSW specimen and corresponding force and moment diagrams as the top beam is pushed to the right. The following assumptions regarding frame behavior at ultimate displacement were made leading to the selection of specimen member sizes. First, in order to test the "anchor" beams concepts discussed above, all frame yielding was assumed to occur in the form of plastic moment hinges at the beam ends, with a value of $\beta \cdot M_p$, where β=fraction of beam strength M_p due to the presence of an RBS connection. Second, a uniform infill panel tension field stress σ is assumed for simplified calculations for preliminary design [that is equivalent to assuming a boundary frame with rigid members and pin-ended connections as illustrated in Fig. 1(b)]. On the basis of that assumption, note that when panel tension field action is discretized into diagonal strips at an angle α, all strips would have the same strain and stress at any given magnitude of frame sway.

Boundary Frames

Following the selection of the 4,000 mm × 2,000 mm frame centerline dimensions described above, frame members were designed using the sequence of steps outlined below, assuming LYS100 infill panel material.

These design steps were preliminarily used to select members assuming simply supported end conditions, then full moment resistant end conditions, and finally 50% (beam) end moment strength reduction. This latter scenario is the case to be considered via experimental testing. The chosen beam and column sections were W18×65 and W18×71, respectively.

The desired limit states for the specimens to achieve at the ultimate condition were: the full development of plastic moment hinges in the beam ends of boundary frame; and full tension field yielding of the infill panel (to the extent typically observed in SPSW testing, within the limits of applicability of the tension strip model). This was implemented in the design by superimposing the frame collapse mechanism case [as shown in Fig. 2(a)] with that of a fully yielded panel [as shown in Fig. 2(b)], exerting a distributed force along the length of each of the surrounding frame members. From simple plastic analysis, the strength of the bare frame (without infill panel) is given by

$$V_{yf} = \frac{4 \cdot \beta \cdot M_p}{\lambda \cdot (H + h_{hinge})} \tag{4}$$

where λ=ratio of the distance between the centerline of the RBS connections and the centerline of the columns; H=frame height between beam centerlines; h_{hinge}=distance from the column base pinned hinge to the bottom beam centerline; and other variables have been defined previously.

Reduced beam section connections were implemented in the specimen design, with a target beam-end moment strength reduction β of 50%. The SAC project (FEMA 2000) criteria, and AISC 358 (AISC 2005a), suggest a maximum beam flange width reduction of 50%, which, due to the contribution of the web to overall section flexural strength, resulted in a design RBS plastic moment strength (452.6 kN m for specified yield strength) that was 60.2% of the span plastic moment strength (752.1 kN m). The resulting connection detail consisted of a 250 mm radius and a flange reduction of 100 mm at the center of the RBS connection [refer to FEMA (2000)].

From previous work (Thorburn et al. 1983), the panel's contribution to the strength of the system is given by

$$V_{yp} = \frac{1}{2} \cdot F_{yp} \cdot t \cdot W_{panel} \cdot \sin 2\alpha \tag{5}$$

where W_{panel}=panel width between column flanges. However, for the specimens considered, the panel's force contribution to the overall system strength must be modified (from geometry) to account for the presence of the hinged base

$$V'_{yp} = \frac{H}{(H + h_{hinge})} \cdot V_{yp} \tag{6}$$

Therefore, the total strength of the system is given by the summation of Eqs. (4) and (6)

$$V_{y\cdot tot} = V_{yf} + V'_{yp} \tag{7}$$

Using these relations and the selected sections and geometry with: h_{hinge}=850 mm, a frame material yield strength of F_{yf} =379.5 MPa [345 MPa (50 ksi) increased by a factor of 1.1 to account for material overstrength], panel thickness and strength of t=2.6 mm and F_{yp}=230 MPa, respectively, the frame and panel contributions to strength are: V_{yf}=941 kN, and V'_{yp}=741 kN, respectively. Total system strength was, therefore, calculated to be 1,682 kN.

A nonlinear static pushover analysis was conducted for an idealized "strip model" using SAP2000 (CSI 2002) for the selected components and the assumed LYS material properties for the

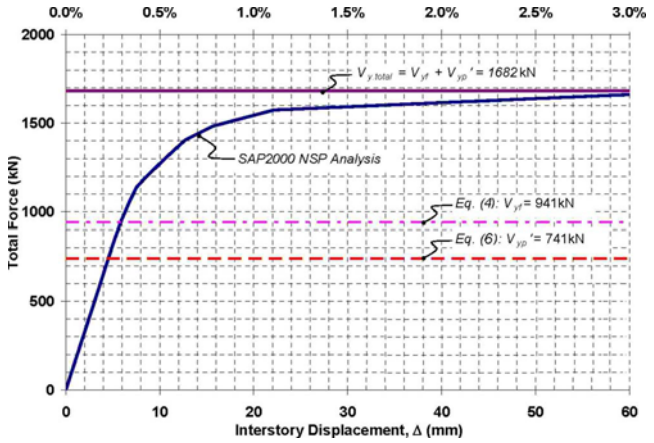

Fig. 3. Pushover analysis and limit calculations

panel to be tested (as described in the next section). The force versus interstory displacement of the SAP model is shown in Fig. 3 along with the values of Eqs. (5)–(7).

To facilitate comparison of the behavior between specimens and quantification of the impact of various infills, all specimens were designed to have the same beams and columns. Frame members were specified to be fabricated from steel equivalent to ASTM A572 with minimum yield strength of 345 MPa. These section sizes were converted to built-up sections with metric measurements, as is the fabrication practice in Taiwan, where the testing occurred. The basic specimen dimensions and infill plate connection detail are shown in Fig. 4. "Fish plates" connecting the infill panel to the boundary frame were designed using simple capacity design principles. The plate was attached to beam and column flanges using fillet welds on both sides of the plate as shown in Fig. 4(b).

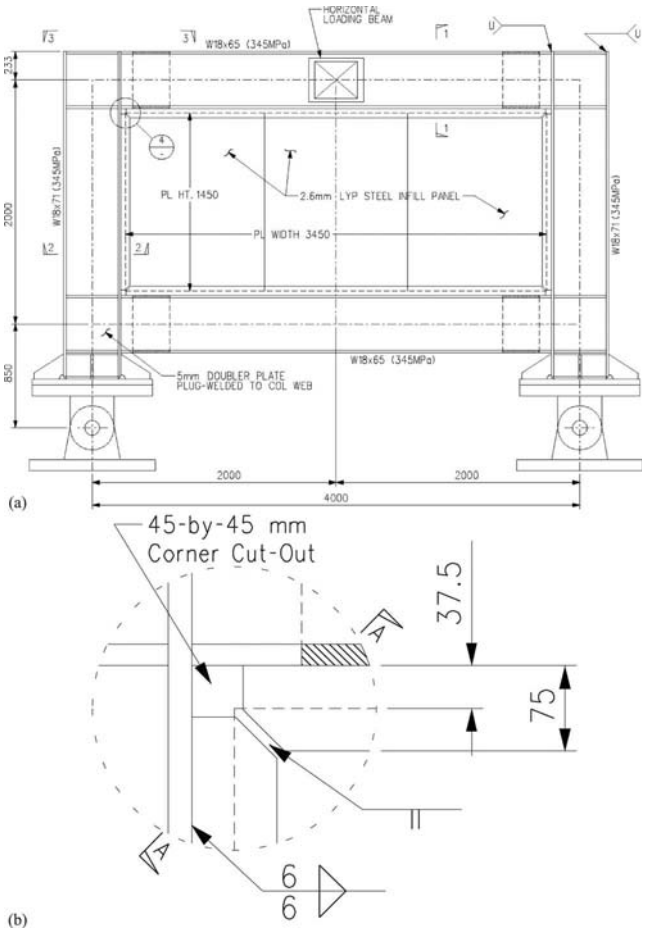

Fig. 4. Basic S specimen: (a) dimensions; (b) fishplate corner detail (dimensions in mm)

Infill Panels LYS Steel

The China Steel Company provided LYS panels of 2.6 mm thickness, in 2,000 mm by 1,230 mm sections, with yield and ultimate stresses of 165 and 305 MPa, respectively. Results from uniaxial tension tests of four panel coupons are shown in Fig. 5, two each cut transverse (T1 and T2) and longitudinal (L1 and L2) to the direction of rolling. Three panel sections were joined manually by the fabricator with "seam welds" using E7018 electrodes at section interfaces, approximately located at the third points (between column faces) of beam clear span in the completed specimens. This "seam welding" was performed prior to installation in the framing to ensure the panel was as flat as possible.

Perforated Panel Specimen (P)

An option for allowing the passage of utilities through an SPSW infill panel via perforations was discussed previously. To design such a specimen, an equation quantifying panel stiffness reduction due to the presence of perforations was derived, while the strength reduction was estimated using the equation proposed by Roberts and Sabouri-Ghomi (1992).

Tension field action in SPSW panels is typically oriented at an angle α near 45° with respect to the surrounding frame (Driver et al. 1997). Therefore, this value was selected as the orientation angle for layout of diagonal strips and perforations in the perforated panel specimen. The number of rows N_r, diameter D, and spacing of the perforations S_{diag}, and the expected effective panel stiffness reduction K_{perf}/K_{panel} were determined through iteration using the following relationship (Vian and Bruneau 2005) for a panel height H_{panel}, equal to 1,534 mm (same as for the solid panel specimen above):

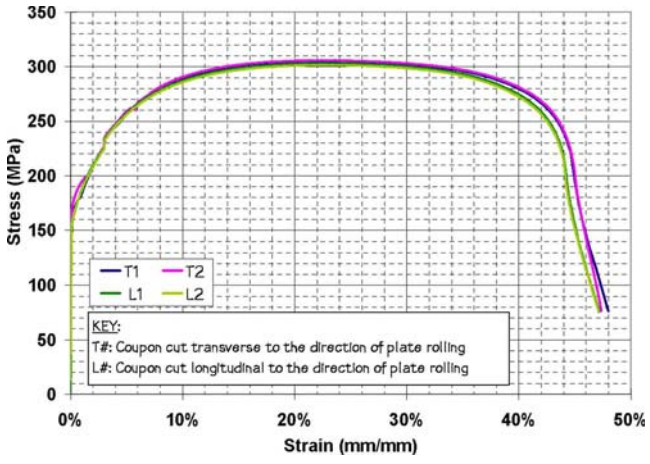

Fig. 5. Low-yield strength steel coupon results

$$\frac{K_{perf}}{K_{panel}} = \frac{w_{eff}}{S_{diag}} = \frac{1 - \frac{\pi}{4} \cdot \left(\frac{D}{S_{diag}}\right)}{1 - \frac{\pi}{4} \cdot \left(\frac{D}{S_{diag}}\right) \cdot \left(1 - \frac{N_r \cdot D \cdot \sin\theta}{H_{panel}}\right)} \quad (8)$$

where w_{eff}=effective width of a perforated diagonal infill panel strip, and θ=orientation angle of a perforated strip, with respect to the horizontal. For practical purposes, a perforation diameter of 200 mm was deemed to provide a suitable size hole for the half-scale specimen, allowing for the passage of a 350 mm (14 in.) diameter water conduit (for example) through the corresponding 400 mm full size hole in the prototype. Therefore, to uniformly fill the panel with perforations of that diameter, N_r equal to 4 was selected as the basis for a final specimen design. This choice provided a balance in perforation layout concerns, with the diagonal spacing slightly less than twice the perforation diameter, and the layout was estimated to provide a significant amount of stiffness reduction (23.5% less stiff compared with a solid panel) according to the relations developed in the previous section. The final design deviated slightly to account for ease of fabrication, resulting in a horizontal and vertical perforation spacing of 300 mm, or S_{diag} of 424.26 mm (300/sin 45°). This alteration decreased the ratio D/S_{diag} to 0.4714 (with an estimated stiffness reduction of 17.8%) by slightly reducing the edge distance to approximately $1.6D$.

Cutout Corner-Reinforced Panel Specimen (CR)

Cutout corner SPSWs were presented as another option for allowing utility passage through an SPSW infill panel. While providing utility access, this proposed system was expected to provide strength and stiffness similar to a solid panel SPSW system by situating a large opening immediately adjacent to the column in each of the top corners of the panel, a location where large utilities are often located (John Hooper, Principal and Director of earthquake engineering Magnusson Klemencic Associates, Seattle, Wash., personal communication, 2006). In designing the plate reinforcing the corner cutout as a semicircular arch, it was recognized that:

1. Whether hinges at arch connections to the beam and column were actual hinges or plastic moment hinges, the arch would resist the infill panel tension load until development of a plastic collapse mechanism with a midspan plastic hinge;
2. For arches with hinged ends, axial load and bending moment at the arch midpoint under thrusting action (Leontovich 1959) due to change of angle at the corner of the SPSW can be expressed as a function of SPSW drift γ by Eqs. (9) and (10), respectively, as

$$P_{frame\text{-}pin} = \frac{15 \cdot E \cdot I}{4 \cdot (2 - \sqrt{2})^2 \cdot R^2} \cdot \gamma \quad (9)$$

$$M_{frame.CL} = \frac{15 \cdot E \cdot I}{8 \cdot (2 - \sqrt{2}) \cdot R} \cdot \gamma \quad (10)$$

3. An expression for the maximum arch plate section thickness at mid span can be obtained by substituting Eqs. (9) and (10) into the axial-moment interaction equation for the reinforcing plate.

From these considerations, and by considering a maximum SPSW drift of 4% and 345 MPa material yield stress, the required maximum thickness of the "opening" corner arch [top left side of Fig. 2(a), with no panel stresses assumed to be acting on it] was calculated to be 19.5 mm. Note that the arch plate width is not a parameter that enters the solution of the interaction equation in that calculation. The required arch plate width is conservatively obtained by considering the strength required to resist the axial component of force in the arch due to the panel forces at the closing corner [top right side of Fig. 2(a)]. Since the components of arch forces due to panel forces are opposing those due to frame corner opening, the actual forces acting in the arch plate will be smaller than calculated by considering the components individually as done above for design.

A fish plate was then added to the selected plate to facilitate infill panel attachment to the arch. It was recognized that this addition would result in a stiffer arch section, and it was estimated that, due to compatibility of frame corner deformation, it would be possible to yield part of this "T" at 4% drift under corner opening. However, because the thickness selected per the procedure outlined above was considered robust enough to withstand the loads alone, it was assumed that the presence of the stiffer and stronger T section would not be detrimental to the system performance.

The resulting arch cross section was 160 mm wide by 19 mm thick, with a 6 mm by 45 mm fish plate. Again, nonlinear static pushover analysis was performed on a model design according to the previously outlined steps using SAP2000 to confirm that the selected section did not produce an undesirable "knee-brace effect" or precipitate column yielding or beam yielding outside of the RBS region. Further details in this design concept are provided in Vian and Bruneau (2005).

Test Setup

Photographs of specimens P, CR, and S2 taken prior to testing are presented in Fig. 6, including supporting hinges, lateral supports, and loading apparatus, as described below.

Each specimen was supported by two hinges located at the base of the columns [see Fig. 4(a)], each of 3,000 kN capacity, and fastened to the strong floor of the laboratory using high strength, posttensioned rods. Specimen column base plates and spacers were dimensioned such that the hinge axis was 850 mm from the centerline of the bottom beam [i.e., the distance h_{hinge} referenced above and shown in Fig. 2(a)].

An existing "H" shaped loading apparatus used in previous experiments performed in the NCREE facility was utilized for this testing program. This apparatus allowed for the attachment of four actuators in parallel for applying the load to the specimen via the center of the top beam. The horizontal box beam of the H was fabricated into each specimen, by welding it to the top beam's web and flanges. The two vertical legs of the H were then connected to the box beam, using high strength bolts, after each specimen was moved into the testing bay and affixed to the column base plates. Actuators were then bolted to the concrete reaction wall and the legs of the H loading detail, as shown in Figs. 6(a and c).

Lateral support was provided at three locations along the top beam of each specimen. Additional framing provided lateral supports at each column, while the loading detail itself provided some degree of lateral support at the center of the beam, as shown in Fig. 6.

Instrumentation

A combination of instruments were used to capture the response of the boundary frame and the infill panels, including: magneto-

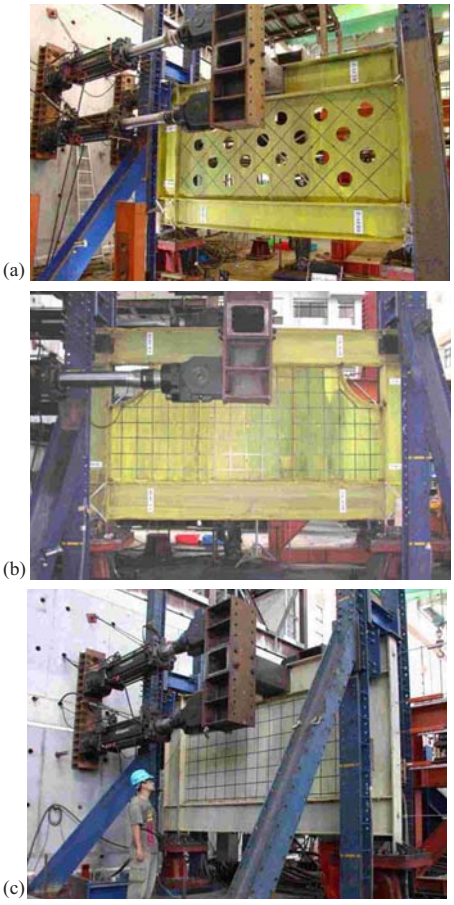

Fig. 6. Photographs of specimen prior to testing: (a) P; (b) CR; and (c) S2

strictive displacement transducers, linear potentiometers, and numerous strain gauges. The applied load was obtained directly from the loading actuators.

Displacements were measured at a number of locations on the specimen. The displacement transducers were utilized for measurement of horizontal displacements at the centerline of the top and bottom beams. Linear potentiometers were used to measure horizontal displacements at the quarter points along the height of the far column, with respect to a fixed reference instrumentation column and along the diagonal.

Additionally, panel behavior was measured qualitatively by means of a visible "grid" on each specimen, which allowed for simple observations of buckling orientation and yielding locations (via the flaking whitewash) in the panel during testing. Gridlines were spaced at 200 mm horizontally and vertically on specimens CR and S2, while on specimen P, gridlines were centered between diagonal strips of perforations, as shown in Fig. 6.

Loading Program/Protocol

The tests were conducted using displacement-controlled quasi-static cyclic loading. As such, the loading protocol was developed as a hybrid/combination of the ATC-24 (ATC 1992) protocol and the AISC Seismic Provisions (AISC 2005b) requirements for loading sequence in cyclic testing.

After panel and frame material coupon testing data were received, a pushover analysis was performed using SAP2000 on the previously described "strip" model of the solid panel specimen

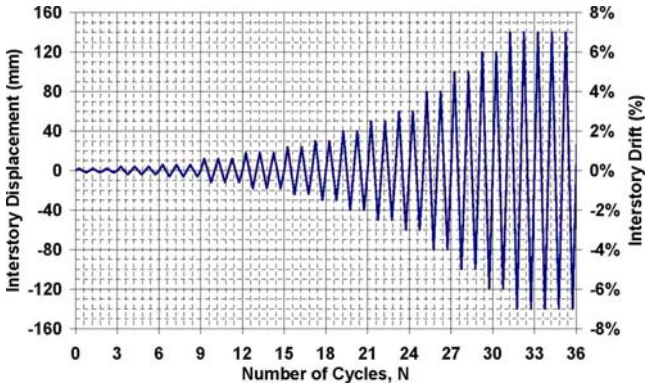

Fig. 7. Loading history

with as-built properties to estimate the global yield force and displacement values, and to establish the specimen loading cycle amplitudes.

Values of the initial two displacement amplitudes were chosen as $\frac{1}{3}$ and $\frac{2}{3}$ of the estimated yield displacement (corresponding to interstory drift amplitudes of 0.1 and 0.2%) to ensure observation of multiple elastic cycles prior to the specimen reaching the global inelastic region of behavior. Three cycles were to be performed at each of these amplitudes, in compliance with the ATC 24 loading protocol (ATC 1992) recommendation of a minimum of six cycles at amplitudes less than δ_y (although it suggests using force control up to a force level of approximately $0.75Q_y$). Once the three cycles at the estimated yield displacement were completed, maximum displacements were increased by multiples of δ_y until reaching an estimated ductility of three. After this point, the number of cycles at each target displacement was decreased from three to two, and these target values continued to increase by an estimated ductility of one until a ductility of five was reached. This estimated ductility coincided with a 1.5% story drift as measured from displacement of the top and bottom beams. Beyond this point, cycle amplitudes were increased by drift increments of 0.5% until reaching 3.0%, and increments of 1.0%, subsequently. Fig. 7 shows the resulting values for the target loading history, with the interstory displacement magnitude on the left vertical axis, and corresponding interstory drift on the right vertical axis.

Experimental Results and Observations

Hysteresis plots of specimen base shear versus interstory displacement are shown for specimens P, CR, and S2 in Fig. 8. Fig. 9 presents photographs of specimens P, CR, and S2 taken during testing at 3, 4, and 3% drift, respectively.

Specimen P

Testing of perforated panel specimen P began with three cycles each at interstory drift amplitudes of 0.1 and 0.2% (corresponding to estimated values of $1/3\ \delta_y$ and $2/3\ \delta_y$). Elastic buckling of the panel and linear force-displacement behavior was observed. The observed elastic stiffness was approximately 115 kN/mm. Panel yielding was first observed after cycle drift amplitudes were increased to 0.3% ($\approx 1\ \delta_y$), as base shear reached 850 kN. Flaking of whitewash was noted between perforations at two locations on the panel corroborating attainment of yield displacement at drift values predicted from the pushover analysis. Cyclic drift ampli-

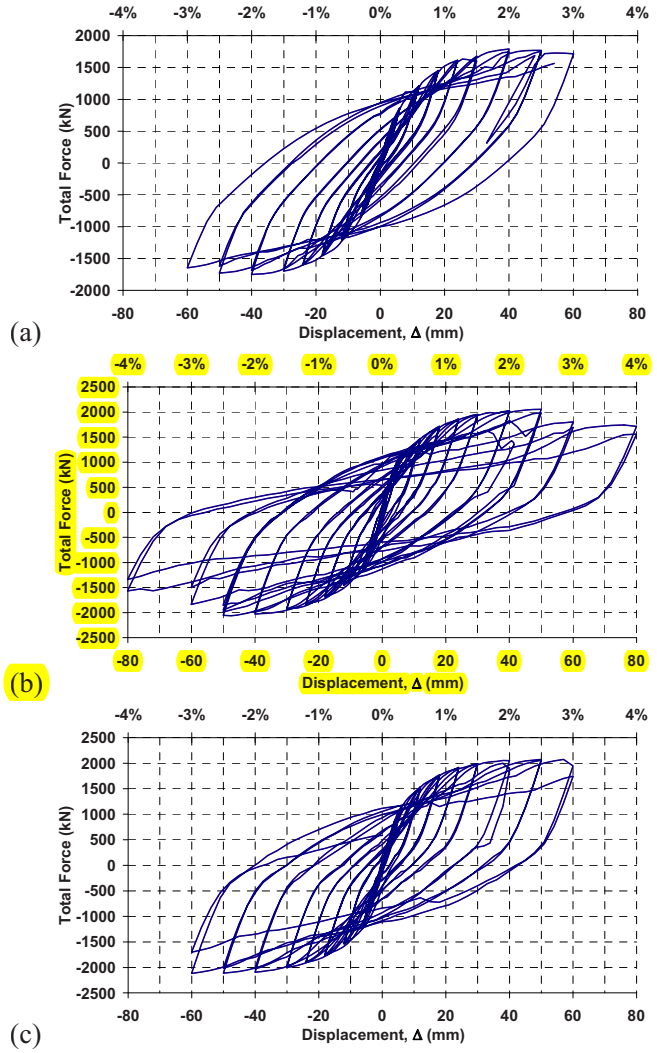

Fig. 8. Specimen hysteresis: (a) P; (b) CR; and (c) S2

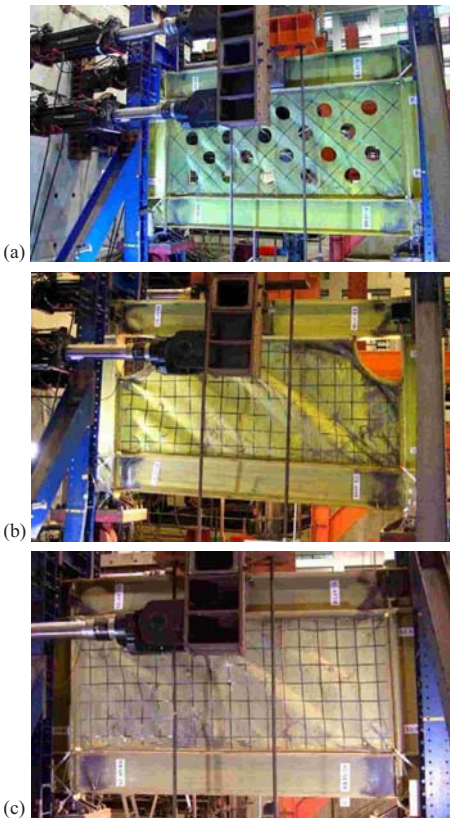

Fig. 9. Photographs of specimen: (a) P at 3% drift; (b) CR at 4% drift; and (c) S2 at 3% drift

tudes were increased incrementally from 0.6% ($\approx 2\ \delta_y$) to 2.0% ($\approx 6.67\ \delta_y$) resulting in maximum peak base shear values of approximately 1,200 and 1,770 kN, respectively. During cycling, yielding progressed throughout the panel and the RBS connections as evidenced by flaking of the whitewash. Additionally, the H loading assembly began to rotate within its plane up to approximately 4°, twisting the top beam at the midspan point of attachment.

Cycling, however, continued to a drift amplitude of 2.5% ($\approx 8.33\delta_y$) resulting in a slight decrease in base shear, to approximately 1,750 kN. Twisting of the loading beam increased once again, and as a result, the top of the wall column was observed to have twisted about its longitudinal axis, causing damage to the lateral support at that location. Rotation also occurred in the far column, as evidenced by the slip of the lateral support plate located on top of the columns.

Testing continued with cycles at 3.0% drift amplitude ($\approx 10\ \delta_y$). The peak base shear continued to decrease, with values of 1,715 and 1,650 kN at the positive and negative peaks of the first cycle, respectively.

Testing was concluded after an audible bang was heard and a drop occurred in the strength of the specimen during the second positive displacement excursion. Subsequent inspection revealed a continuity plate fracture on the far column at the wall flange. Flange local buckling was observed in the bottom flange of the far bottom beam RBS connection. Although the steel plate wall had not yet fractured (beyond the continuity plate problem indicated above), damage and distortions of the boundary frame made it impractical to continue testing.

Specimen CR

Prior to the testing of specimen CR, the lateral support system provided at the top of each column was modified in an attempt to prevent column twist observed during testing of the specimen P.

Testing of the CR specimen began with three cycles each at 0.1 and 0.2% drift amplitudes, producing peak base shears of approximately 550 and 900 kN, respectively. Elastic buckling was observed in the panel during the 0.1% drift cycles, with no visible signs of yield. Following the first cycle at 0.2% drift amplitude, a slight flaking of the whitewash was observed in the web of the far column, near the bottom beam. After the remaining two cycles at this amplitude, slight whitewash flaking was visible near the top flange of both bottom beam RBS connections.

Cycle drift amplitude was then increased to 0.3%, the estimated yield drift in the pretest analyses ($\approx 1.0\ \delta_y$). The specimen resisted this displacement with a base shear of approximately 1,125 kN. The observed elastic stiffness was approximately 140 kN/mm. Yield lines appeared in a number of locations near the far column and top beams on the panel. Small yield lines appeared on the web of the far side top beam RBS connection. Again, cyclic drift amplitudes were incrementally increased from 0.6% ($\approx 2.0\ \delta_y$) to 3.0% ($\approx 10.0\ \delta_y$), resulting in maximum peak base shear values of approximately 1,470 and 2,060 kN, respectively. During cycling between these drift amplitudes, yielding

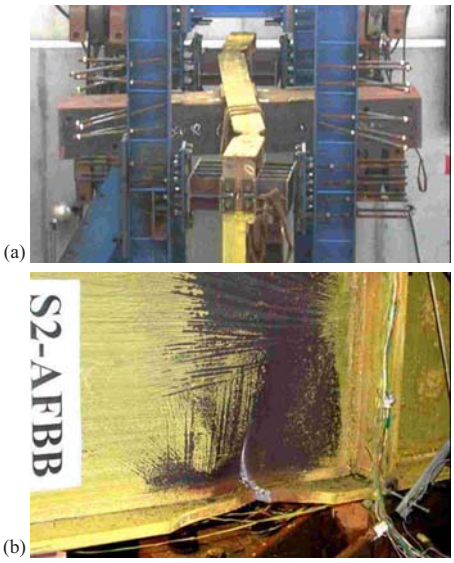

Fig. 10. Photographs taken upon completion of testing: (a) longitudinal view of specimen CR; (b) rupture of bottom beam RBS connection of specimen S2

progressed in the panel and the RBS connections. During the second cycle at 3.0% drift, the far side bottom beam RBS bottom flange fractured at two points, further reducing the specimen strength to 1,700 and 1,500 kN at the positive and negative peaks, respectively.

Loading displacement increased to 4.0% drift amplitude ($\approx$13.33 δ_y), which produced specimen strengths of approximately 1,750 and 1,560 kN, during the positive and negative excursions of the first cycle, respectively. Audible bangs were heard during the cycles at this amplitude and during the second cycle, specimen strengths during the positive and negative excursions reduced to approximately 1,560 and 1,340 kN, respectively. These strength values correspond to drops of 24 and 35% from the positive and negative strength peaks for the duration of the test, respectively.

The overall behavior of the specimen suggested that it could continue to resist loading to larger displacements. However, testing was concluded to prevent lateral support damage that may have occurred due to twisting of the columns as shown in the photograph of specimen CR taken at the conclusion of testing; see Fig. 10(a). Column yielding was observed in a number of locations. Yielding of the continuity plate at the bottom beam top flange and the adjacent far column web had increased as the test progressed. The upper portion of the far column exhibited yielding of the wall flange (adjacent to the corner cutout-reinforced arch), as well as the web from the top beam bottom flange continuity plate to the region near the lower end of the arch. Similar yielding patterns were observed in the wall column.

Specimen S2

Testing of the solid panel specimen S2 was carried out using the same methodology as implemented for specimen CR. Testing began with three cycles at 0.1% drift amplitude, which resulted in a peak base shear of approximately 500 kN, with no visible signs of yield. Three cycles at 0.2% drift amplitude were next applied to the specimen. A peak base shear of 900 kN was observed, with elastic behavior for the first cycle. Yield lines in the flaked whitewash were noted on the webs at the bottom of the far and wall columns.

Cycle drift amplitude was then increased to 0.3%, the estimated yield drift in the pretest analyses ($\approx$1.0 δ_y). The peak base shear was approximately 1,150 kN corresponding to an elastic stiffness of approximately 130 kN/mm. Again, cyclic drift amplitudes were incrementally increased from 0.6% ($\approx$2.0 δ_y) to 2.5% ($\approx$8.33 δ_y) with the maximum base shear increasing from approximately 1,500 to 2,085 kN, respectively. Following the cycles at 2.5% drift amplitude, yield lines were noted in the top beam web, near the horizontal beam of the loading detail. A crack was found in the continuity plate weld on the bottom beam bottom flange at the far column wall flange. Cracks were noted at both panel corners at the wall column. Bottom beam wall RBS connection web local buckling worsened and bottom flange local buckling become more evident. Yielding increased at the top of the column webs, in the top beam panel zones, and the adjacent top beam bottom flange continuity plates. By this point, however, the top beam distorted in its horizontal plane, as occurred in previous specimen tests [see Fig. 10(a)]. The bottom beam continuity plate weld crack at the far column grew in size and a small crack was found in the bottom flange of the bottom beam far RBS

Cycle drift amplitude was increased to 3.0% ($\approx$10.0 δ_y) for two cycles. A 15% strength reduction occurred during the second positive excursion at this drift amplitude, after a fracture of the bottom beam wall RBS bottom flange, which spread into the web as the specimen approached the peak displacement. During the second cycle at 3.0% drift amplitude, a 20% drop in strength at the peak of the negative excursion resulted from the fracture of the bottom beam far RBS bottom flange, as shown in Fig. 10(b). In addition, the cracked continuity plate weld adjacent to this connection had fully fractured by the end of the second cycle at 3.0% drift amplitude. Testing ceased after completion of the second cycle. The specimen columns had twisted severely about their respective axes, and the top beam was bent out of plane in an "S" shape.

Column yielding had increased substantially in the far column web, wall flange, and adjacent bottom beam top flange continuity plate by the conclusion of testing. Infill panel damage across the entire panel consisted of tension yielding and folds from buckling, as well as cracks at the corners.

Comparison of Results

The values of peak base shear strength, ductility, drift, and elastic stiffness are summarized for each specimen in Table 1. Specimen P, containing 20 circular perforations in the infill panel, was successfully tested to a maximum interstory displacement of 60 mm (3%, 10 δ_y) and maximum base shear of 1,790 kN at 2% drift. The specimen strength and elastic stiffness were approximately 15% lower than the values obtained for the solid panel specimen (S2) at comparable drift levels. Specimen CR, having reinforced quarter-circle cutouts in the panel corners, was successfully tested to a maximum interstory displacement of 80 mm (4%, 13.33 δ_y) and maximum base shear of 2,050 kN at 2.5% drift. At the peak displacement, the overall specimen strength had dropped by an average of 30% from the peak value, following fracture of the bottom flange in both bottom beam RBS connections. Specimen S2, a solid infill panel specimen, was successfully tested to a maximum interstory displacement of 60 mm (3%, 10 δ_y) and maximum base shear of 2,115 kN at −3% drift. Specimen

Table 1. Summary of Peak Results

Specimen	Elastic stiffness (kN/mm)	Maximum base shear strength (kN)	Approximate maximum displacement ductility ($\mu=\Delta/\Delta y$)	Maximum interstory drift (%)	Strength reduction at maximum drift (%)
P	115	1,790	10	3	14.5
CR	140	2,050	13.33	4	30
S2	135.5	2,115	10	3	18

strength had reduced by an average of 18% at the conclusion of testing, due to fracture of the bottom flange of each bottom beam RBS connection.

In all cases, although the specimens could resist significant loads up to larger displacements after a redistribution of the load path from that of the virgin specimen, testing stopped because significant fractures had occurred in the bottom beam RBS and the top beam and top of the columns had twisted severely (damaging the lateral supports at those locations in some cases). These failures, partly attributed to shortcomings in the test setup, nonetheless occurred at drift values beyond the expected drift demands for structural systems having such large stiffness, and did not impact performance of the system until then. Furthermore, presence of floor slabs in an actual building could help delay the onset of these failures.

Summary and Conclusions

Two proposed methods for allowing passage of utilities through SPSWs were tested in the experimental program. One method slightly alters a solid panel by introducing a reinforced, quarter-circle cutout into each upper corner of the infill panel. This system is intended to transfer the full panel diagonal tension field forces to the boundary frame and, therefore, provide the same overall strength as a solid panel, while simultaneously providing a means for utilities to penetrate the infill, as required in a retrofit or new design situation. A simple method was presented for the preliminary design of these reinforcement members.

Another proposed system introduces multiple circular perforations, arranged in regularly spaced diagonal strips within the perimeter of the infill panel. This system would allow utility pass through, while also serving as a means of reducing the strength and stiffness of a solid panel uniformly throughout the panel by distributing the effects of perforations throughout the panel tension stress field. This option may be beneficial to designers who feel an SPSW system is suited to a particular structure, but the required solid infill thickness is unreasonably small. A method of estimating strength reduction due to the presence of a single perforation within a panel, as presented in past research, was discussed as suitable for this system.

An experimental program was designed to investigate the above utility-accommodating concepts, along with the introduction of RBS in anchor beams. In addition, these experiments implemented low yield strength (LYS) steel into an SPSW for the first time. Quasi-static, cyclic testing was carried out on three single-story, single-bay specimens, of approximately half-scale in size.

Each system behaved in a ductile manner, with load-path redundancy within the panel, resisting imposed displacement loading to a drift of 3% or greater. In all cases, beam plastic hinging was located in the RBS at the beams' ends. The RBS design concept ensured that the beams could continue to "anchor" the infill panel tension field forces without developing a collapse mechanism with midspan plastic hinging that could compromise the overall system strength. The results of the experimental investigation suggest the RBS connection is an effective detail for SPSW anchor beams and is recommended to control boundary frame yielding during a significant earthquake.

The special perforated panel SPSW specimen with multiple regularly spaced holes exhibited ductile behavior during testing and is a viable alternative to a solid panel SPSW, to allow utility access through the panel without the need for stiffeners around the perforations, as required by current seismic design specifications (AISC 2005b). This system is also recommended for use in SPSW applications where the minimum available plate thickness is larger than the required, allowing the effective strength of the solid panel to be reduced and minimizing force and moment demand (from capacity design) on the surrounding frame. The cutout reinforced corner system also performed well during testing and appears to be an effective solution for SPSW implementation allowing for the passage of utilities at panel corners near to the columns. The above findings should not be implied to remain valid for SPSW having random perforation patterns or holes of different geometries—further research would be necessary to investigate such special cases that substantially differ from the special systems considered here.

Acknowledgments

This work was supported in part by the Earthquake Engineering Research Centers Program of the National Science Foundation under Award No. ECC-9701471 to the Multidisciplinary Center for Earthquake Engineering Research. The assistance of Dr. Gordon Warn during manuscript preparation is also appreciated. However, any opinions, findings, conclusions, and recommendations presented in this paper are those of the writers and do not necessarily reflect the views of the sponsors.

References

AISC. (2005a). "Prequalified connections for special and intermediate steel moment frames for seismic applications." *ANSI/AISC 358-05*, American Institute of Steel Construction, Inc., Chicago, Ill.

AISC. (2005b). "Seismic provisions for structural steel buildings." *ANSI/AISC 341-05*, American Institute of Steel Construction, Inc., Chicago, Ill.

Applied Technology Council (ATC). (1992). "Guidelines for seismic testing of components of steel structures." *Rep. No. 24*, ATC, Redwood City, Calif.

Berman, J. W., and Bruneau, M. (2003a). "Experimental investigation of light-gauge steel plate shear walls for the seismic retrofit of buildings." *Technical Rep. No. MCEER-03-0001*, Multidisciplinary Center

for Earthquake Engineering Research, Buffalo, N.Y.

Berman, J. W., and Bruneau, M. (2003b). "Plastic analysis and design of steel plate shear walls." *J. Struct. Eng.*, 129(11), 1148–1156.

Berman, J. W., and Bruneau, M. (2005). "Experimental investigation of light-gauge steel plate shear walls." *J. Struct. Eng.*, 131(2), 259–267.

CAN/CSA. (2001). "Limit states design of steel structures." *S16-01*, Canadian Standards Association, Mississauga, Ontario, Canada.

Computers and Structures Inc. (CSI). (2002). *SAP2000: Analysis reference manual*, Ver. 8.0, Berkeley, Calif.

Driver, R. G., Kulak, G. L., Kennedy, D. J. L., and Elwi, A. E. (1997). "Seismic behavior of steel plate shear walls." *Structural Engineering Rep. No. 215*, Dep. of Civil and Environmental Engineering, Univ. of Alberta.

FEMA. (2000). "Recommended seismic design criteria for new steel moment-frame buildings." *FEMA 350*, SAC Joint Venture for the Federal Emergency Management Agency, Washington, D.C.

FEMA. (2003). "FEMA 450: "NEHRP recommended provisions for seismic regulations For new buildings and other structures." *FEMA 450*, Building Seismic Safety Council for the Federal Emergency Management Agency, Washington, D.C.

Leontovich, V. (1959). *Frames and arches: Condensed solutions for structural analysis*, McGraw-Hill, New York.

Roberts, T., and Sabouri-Ghomi, S. (1992). "Hysteretic characteristics of unstiffened perforated steel plate shear panels." *Thin-Walled Struct.*, 14, 139–151.

Sabelli, R., and Bruneau, M. (2006). "Steel plate shear walls." *Steel design guide*, American Institute of Steel Construction, Inc., Chicago, Ill.

Thorburn, L. J., Kulak, G. L., and Montgomery, C. J. (1983). "Analysis of steel plate shear walls." *Structural Engineering Rep. No. 1073*, Dept. of Civil Engineering, Univ. of Alberta, Edmonton, Alberta, Canada.

Timler, P. A., and Kulak, G. L. (1983). "Experimental study of steel plate shear walls." *Structural Engineering Rep. No. 114*, Dept. of Civil Engineering, Univ. of Alberta, Edmonton, Alberta, Canada.

Vian, D., and Bruneau, M. (2005). "Steel plate shear walls for seismic design and retrofit of building structures." *Tech. Rep. No. MCEER-05-0010*, Multidisciplinary Center for Earthquake Engineering Research, State Univ. of New York at Buffalo, Buffalo, N.Y.

Xue, M., and Lu, L.-W. (1994). "Interaction of infilled steel shear wall panels with surrounding frame members." *Proc., 1994 Annual Task Group Technical Session, Structural Stability Research Council: Reports on Current Research Activities*, 339–354.

Yang, T. Y., and Whittaker, A. S. (2002). "MCEER demonstration hospitals—Mathematical models and preliminary results." *Technical Rep.*, Multidisciplinary Center for Earthquake Engineering Research, Univ. at Buffalo, Buffalo, N.Y.